Available online at www.sciencedirect.com

ScienceDirect

Ceramics International 40 (2014) 1155–1164

CERAMICS INTERNATIONAL

www.elsevier.com/locate/ceramint

Microfiltration of oil–water emulsions using low cost ceramic membranes prepared with the uniaxial dry compaction method

Sriharsha Emani, Ramgopal Uppaluri*, Mihir Kumar Purkait**

Department of Chemical Engineering, Indian Institute of Technology, Guwahati, Guwahati 781039, India

Received 23 May 2013; received in revised form 5 June 2013; accepted 30 June 2013
Available online 16 July 2013

Abstract

This work addresses the comparative assessment of uniaxial dry compaction and paste methods for the preparation of low cost ceramic membranes. Kaolin based low cost membranes were fabricated using uniaxial dry compaction with the identified precursor formulation provided by Nandi et al. [5]. Fabricated membranes were characterized and used for the treatment of synthetic oily waste water solutions. It was observed that in comparison with the paste method, the membranes prepared with uniaxial dry compaction method possessed wider pore size distributions. Amongst several membranes, the membrane PM1 fabricated at a pressure of 25 Mpa provided highest flux of 24×10^{-6} m^3/m^2 s and an oil rejection of 95.2% but with a fouling index of 29.47% at a pressure of 206.70 kPa. On the other hand, PM3 membrane provided a lower fouling index of 15.54% at a pressure of 206.70 kPa with a membrane flux of 8×10^{-6} m^3/m^2 s and a rejection of 97.9%. For the obtained membrane morphology and chosen feed concentration, combination of pore blocking models provided best fit to represent flux decline data. High rejection values (80–90%) and good membrane flux (24×10^{-6} m^3/m^2 s) of the fabricated membranes was observed towards the treatment of oil water emulsions using low cost ceramic membranes.

Keywords: Paste; Uniaxial; Emulsion

1. Introduction

Membrane technology offers several advantages for industrial processing schemes. These include compactness, lower cost and ability to process streams with very low feed concentrations. Amongst various industrial process schemes, the treatment of oil–water emulsions is an important problem in process industries. Typically, the feed composition varies from 50 to 1000 mg/L of oil and it is desired to have a product stream with a maximum oil concentration of 10–15 mg/L [1]. Compared to other separation techniques, membrane technology is promising to process waste feed streams with low oil concentration and achieve high separation efficiency (90–99%).

In the recent times, research in the fabrication of low cost ceramic membranes is getting significant attention. Low cost ceramic membranes have been fabricated using various types of clays and zeolite minerals [2–4]. Nandi et al. [5] fabricated disk shaped ceramic membranes (average pore diameter of 0.77 μm, porosity of 42%) using a mixture of kaolin, quartz, calcium carbonate, sodium carbonate, boric acid and sodium metasilicate by the paste method. The permeate flux and rejection was obtained as 15.05×10^{-6} m^3/m^2 s and 98.5% respectively, at a ΔP of 206.80 kPa and 150 mg/L feed oil concentration. Considering PVA as a binder, Monash et al. [6] fabricated low cost ceramic membrane using kaolin, feldspar, quartz, pyrophyllite, ball clay, calcium carbonate and titanium dioxide by adopting the uniaxial dry compaction method. The fabricated membrane possessed an average pore diameter of 0.83 μm and a porosity of 36%. For a feed oil concentration of 200 mg/L, the membrane provided a permeate flux of 2.50×10^{-5} m^3/m^2 s and a rejection of 99%. Using the same fabrication method, Vasanth et al. [7,8] reported precise inorganic precursor formulations (kaolin, quartz, calcium carbonate, sodium carbonate, boric acid and sodium metasilicate) for the fabrication of ceramic membranes (pore size of 1.30 and 1.06 μm and porosity of 30% and 26%). Amongst these membranes, the second membrane was studied for the

*Corresponding author. Tel.:+91 361 258 2260; fax: +91 361 2582291.
**Corresponding author. Tel.:+91 361 2582262; fax: +91 361 2582291.
E-mail addresses: ramgopalu@iitg.ernet.in (R. Uppaluri), mihir@iitg.ernet.in (M.K. Purkait).

0272-8842/$ - see front matter © 2013 Elsevier Ltd and Techna Group S.r.l. All rights reserved.
http://dx.doi.org/10.1016/j.ceramint.2013.06.117

Nomenclature

ΔP	trans membrane pressure diffrential (kPa)
Δt	sampling time (min)
J	permeate flux (m^3/m^2 s)
V	volume of permeate (m^3)
A	effective membrane area (m^2)
C	concentration of oil in the feed (mg/L)
C_p	concentration of oil in the permeate (mg/L)
R	rejection (dimension less)
FI	fouling index (dimension less)
PW_i	corresponds to the pure water hydraulic permeability values for cleaned membrane
PW_f	corresponds to the pure water hydraulic permeability values for fresh membrane
J_0	initial permeate flux (m^3/m^2 s)
k_b	complete pore blocking model constant (s^{-1})
k_c	cake filtration model constant ($s\ m^{-2}$)
k_i	intermediate pore blocking model constant (m^{-1})
k_s	standard pore blocking model constant ($m^{-0.5}\ s^{-0.5}$)
R^2	square of correlation coefficient (dimension less)
$RMSE$	root mean square error (dimension less)

microfiltration of oil water emulsion with a feed oil concentration of 200 mg/L to obtain a permeate flux and oil rejection of 0.65×10^{-4} m^3/m^2 s and 96% respectively at a ΔP of 69 kPa. Abbasi et al. [9] used kaolin, clay and α-alumina powder to fabricate mullite (average pore size of 0.578 μm and porosity of 32%) and mullite–alumina based ceramic membranes and reported a maximum membrane flux and rejection of 244 L/m^2 h and 93.8% respectively, for the mullite membrane.

A critical analysis of the above literatures provides the following observations. Firstly, several compositions have been presented based on trial and error approaches and a comparative assessment of two different methods namely the dry compaction method and the paste method for an identified precursor formulation has not been addressed. Such studies would be useful to understand upon the possible variation in the membrane morphology with variation in the type of the fabrication method. The paste method involves the usage of water which enables flexibility in the elasticity of the green mold and can contribute significantly towards the alteration in the membrane morphological properties. On the other hand, the uniaxial method involves fabrication pressure as an important parameter which can significantly influence the membrane properties and the insitu performance of the membrane for various applications. Recently, we have reported that fabrication pressure in the uniaxial dry compaction method strongly influences membrane morphological parameters and there exists an optimal fabrication pressure that enables the maximization of permeation flux without compromising upon the juice clarity during mosambi juice clarification [10]. Therefore, such comparative assessment between paste and uniaxial dry compaction methods could provide valuable information and serve as a guideline towards scale up related issues. Secondly, it has been reported only by Nandi et al. [5] that any standard single pore blocking models may not be able to represent the pertinent flux decline mechanism throughout the entire range of operation and combination pore blocking models need to be deployed to represent the flux decline data [5] during the MF of oil–water emulsions with feed concentrations varying from 50 to 150 mg/L. Hence, it is important to examine whether such observations have further validity and especially when the feed oil concentration is high (around 400–500 mg/L) and for membranes fabricated using the uniaxial dry compaction method with the same composition. Thirdly, in several works [4,5,7,8,11], fouling indices have not been reported after conducting microfiltration experiments. Considering the above issues, this work addresses the preparation and characterization of low cost ceramic membranes using the uniaxial dry compaction method using the composition reported by Nandi et al. [5]. As stated previously, the major objective of this work is to compare the membrane morphologies obtained from uniaxial dry compaction with that of paste method and their comparative performance during microfiltration (MF) of oil–water emulsion.

2. Experimental

2.1. Ceramic membrane fabrication

Six different ceramic precursors namely kaolin (CDH, India), quartz (Research Lab Fine Chem Industry, India), calcium carbonate (Merck, India), sodium carbonate (Merck, India), boric acid (Merck, India) and sodium metasilicate (CDH, India) have been used without any further purification to fabricate porous ceramic membranes. Amongst these precursors, kaolin provides low plasticity and high refractory properties; quartz contributes to mechanical and thermal stability; carbonates provide porous texture; sodium carbonate and boric acid act as a colloidal agent to improve dispersion properties and sodium metasilicate acts as a binder to induce higher mechanical strength to the membrane.

Using the composition provided by Nandi et al. [11] on a dry basis (40% kaolin, 15% quartz, 25% calcium carbonate, 10% sodium carbonate, 5% boric acid and 5% sodium metasilicate), the initial step in the fabrication procedure involved the preparation of a membrane mold using a hydraulic press (Make: Velan Engineering, Tamilnadu, India). To obtain membranes with distinct membrane morphologies, three different fabrication pressures namely 25, 39, and 73 MPa have been used and the membranes thus obtained are termed as PM1, PM2 and PM3 respectively. Further procedure involves steps similar to those presented by Nandi et al. [11], except for the drying step. The procedure involves drying of prepared membranes (56 mm diameter and 5 mm thickness) at 150 °C for 24 h to remove adsorbed moisture and subsequent sintering at 900 °C for 4 h with a heating rate of 2 °C/min in a muffle furnace. Eventually, the membranes were allowed to cool in the furnace to 25 °C by

switching the power off. The final steps in the membrane fabrication involves polishing the membrane using C-220 silicon carbide abrasive paper followed with cleaning using Millipore water in an ultrasonic cleaning bath (Make: Elma) (India, Model: T460) for 15 min. It is worthy to mention here that the spent adsorbent used for dye removal [12–14] may be utilized as one of raw material composition for the fabrication of inorganic membrane.

2.2. Membrane characterization

Membrane characterization involves X-ray diffraction (XRD, Make: BRUKER, Model No. D8 Advance, Germany), field emission scanning electron microscopy (FESEM, Make: ZEISS, Model no. ∑IGMA, USA), porosity measurement, hydraulic permeability measurement and measurement of acidic and basic media corrosion resistances. Both hydraulic permeability and microfiltration experiments are carried out in a dead end MF setup made with stainless steel. All experiments are conducted at pressure differentials varying from 68.9 to 206.7 kPa for hydraulic permeability and 137.8–206.7 kPa for MF experiments. Further details with respect to the adopted procedures have been presented elsewhere [10].

2.3. Microfiltration experiments

Synthetic oil–water emulsions with a concentration of 400 mg/L have been prepared using crude oil collected from Guwahati Refinery, Indian Oil Corporation Limited (IOCL), India and millipore water. The emulsifications are carried out in a sonicator (Make: Elma (India); model: T460) for about 15 h without using external emulsifying agents. The prepared emulsions have been used for the MF experiments within one week. Prior to each dead end MF experiment, the feed concentration was evaluated by measuring the absorbance using UV–vis spectrophotometer (Spectra scan, UV 2300) at a wave length of 235 nm, where the maximum absorbance was observed. The MF experiments conducted at 25 °C involves the measurement of permeate volume at an interval of 1 min during a total run time of 30 min, after which nearly steady state flux values have been observed. Eventually, the permeate collected is also analyzed using the spectrophotometer to determine the oil concentration in the permeate stream. The time dependent concentrations in the permeate stream have been obtained by analyzing permeate samples obtained at an interval of 5 min during the MF run. For all the membranes (PM1, PM2 and PM3) the permeate flux (J, m^3/m^2 s) and the percent oil rejection (R) are evaluated using the expressions

$$J = \frac{V}{A \times \Delta t} \tag{1}$$

$$R = \left(1 - \frac{C_P}{C}\right)100 \tag{2}$$

where, A (m^2) is the effective membrane area, V (m^3) is the volume of permeate, Δt (s) is the sampling time, C (mg/L) and C_P (mg/L) are the concentrations of oil in the feed and permeate, respectively.

2.4. Fouling studies

After each MF run, membrane cleaning is carried out by sequentially washing the membrane with tap water for 5 min. Membrane cleaning is done by soaking the fouled membrane in commercial detergent solution (surf excel with a concentration of 2 g/L) for 30 min; tap water washing for 5 min and back flushing; soaking the cleaned membrane in de-ionized water for 15 min and rinsing the membrane with deionized water for 5 min. Following these steps, the membrane is evaluated for its hydraulic permeability. Using the measured hydraulic permeabilities of the fresh and cleaned membranes, the fouling index (FI) is calculated. FI for various membranes is defined as

$$FI = \frac{PW_i - PW_f}{PW_i}100 \tag{3}$$

where, PW_i and PW_f correspond to the pure water hydraulic permeability values for the fresh and the cleaned membranes, respectively. Thus, higher fouling index indicates higher irreversible fouling of the membrane which could be due to pore blocking phenomena. Hence, fouling indices can be used as an additional criterion to opine upon the optimality of various fabricated membranes (PM1, PM2 and PM3) and operating pressures for the treatment of oil–water emulsion.

3. Fouling mechanism

Standard pore blocking models provided by Hermia [15] have been deployed to represent the pertinent flux decline mechanism during MF. Four different models namely cake filtration, intermediate, standard and complete pore blocking models have been evaluated for their fitness to represent the present MF data. Both single and combination modeling approaches have been followed. Further details with respect to the procedures involved have been presented elsewhere [10]. The combination models have been tested by considering the fitness of two different models to represent the short term flux decline (1–10 min) and the long term flux decline (11–30 min) of the MF data. For all cases, the coefficient of correlation (R^2) and RMS error have been used as the basis to identify the most competent model(s). Conceptually, the onset of cake filtration is beneficial from a fouling perspective, as cake filtration may correspond to maximum reversible fouling and is indicative towards longer shelf life of the membrane. In contrast, the fitness of other pore blocking models is indicative towards irreversible fouling scenarios during MF, which could contribute to the shorter shelf life of the membrane and its durability.

4. Results and discussion

4.1. Membrane characterization

Fig. 1 presents the XRD peaks for the unsintered raw material mixture used to fabricate PM3 membrane. It can be observed that quartz, inyoite, kaolin, nepheline peaks exist for

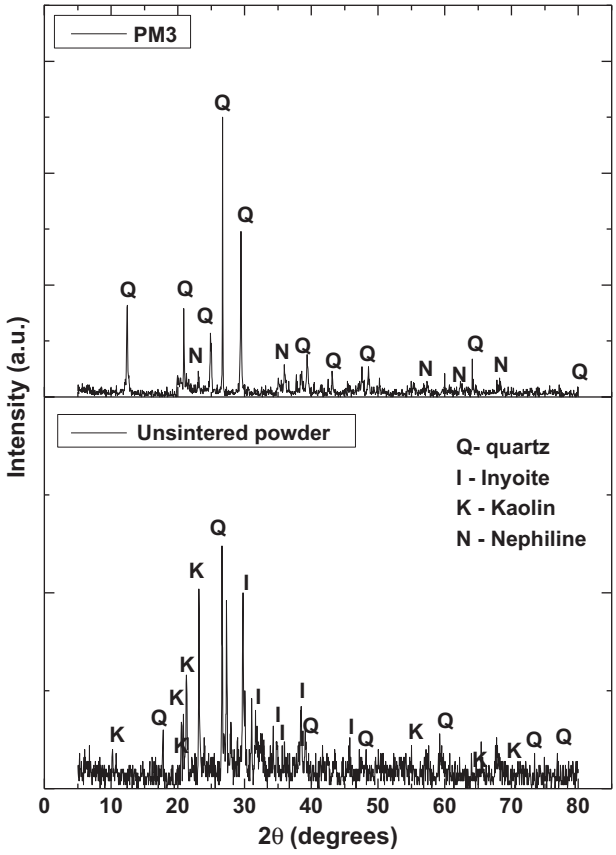

Fig. 1. X-ray diffraction patterns of the raw material mixture for PM3 membrane.

the PM3 membrane. The obtained XRD pattern is in agreement with the XRD pattern obtained by Nandi et al. [11]. Thus, it is apparent that the sintering process enables the conversion of kaolinite to metakaolinite along with the appearance of nepheline phase. Fig. 2(a–c) illustrates the FESEM images obtained from membranes PM1–PM3 respectively. Using Image J software, the pore size distributions of various membranes PM1–PM3 have been obtained and are presented in Fig. 3. It can be observed that the membranes had distinct porous structure with pores ranging from 2 to 10 μm. It may also be seen from the figure that the pore size distributions involve single peak profile with wider pore size distribution for the membrane fabricated at lower pressure. Using these pore size distributions, the average pore sizes of various membranes are evaluated as 3.23 μm, 2.45 μm and 2.33 μm for PM1, PM2 and PM3 membranes, respectively. Further, it can also be observed that the maximum number of pores (%) varied significantly with fabrication pressure and are 35%, 26%, and 20% for PM1, PM2 and PM3 membranes, respectively. In this regard, it can be analyzed from the data trends presented by Nandi et al. [5] that the pore size distributions of the membranes fabricated by the paste method varied from 0.1 to 3 μm with 25% pores possessing a pore diameter of about 0.5 μm. The average pore size of the membrane is 0.55 μm. Thus, it is apparent that the uniaxial dry compaction method provides membrane with significantly wider pore size distribution than the membrane obtained with the paste method. This

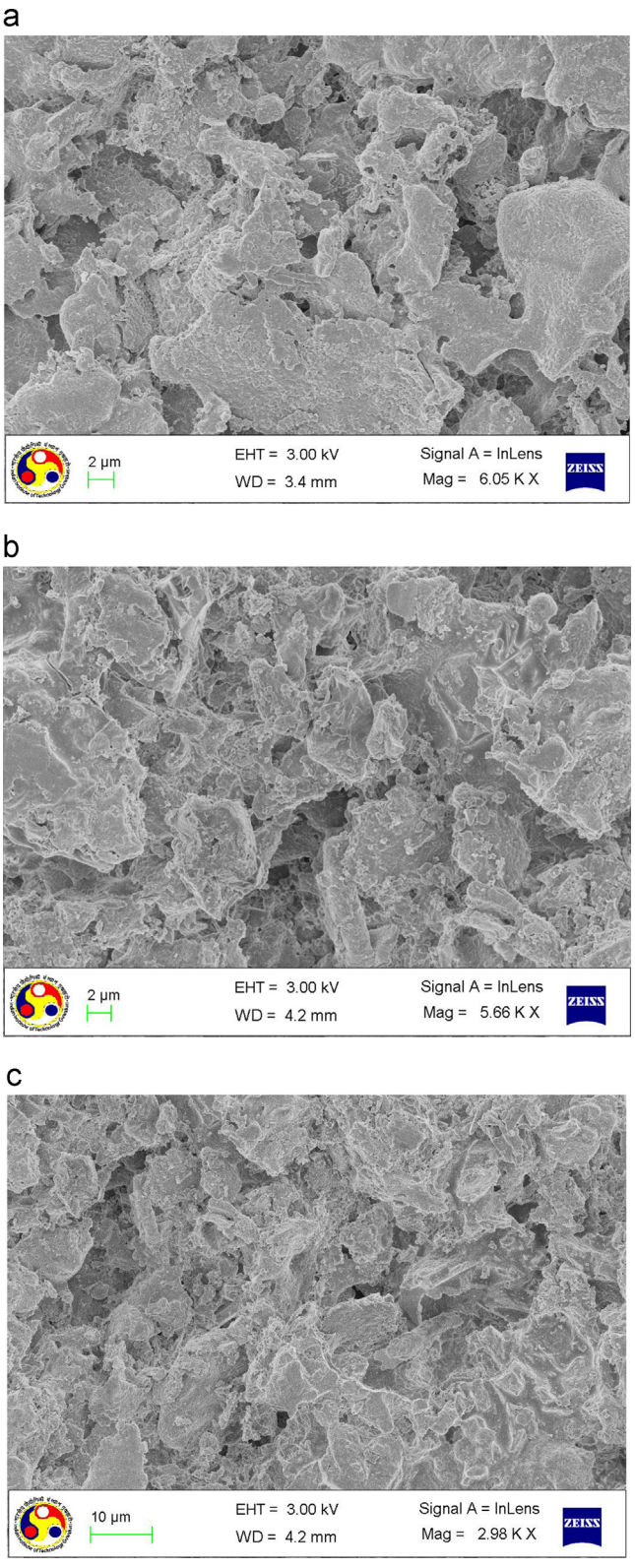

Fig. 2. FESEM images of PM1, PM2 and PM3 membranes.

is a very important observation given the fact that the presence or absence of water strongly influences plasticity of the green mold and hence membrane morphology after sintering. The variations of pure water flux for various membranes are presented in Fig. 4a. The pure water flux varied from 3.16 to

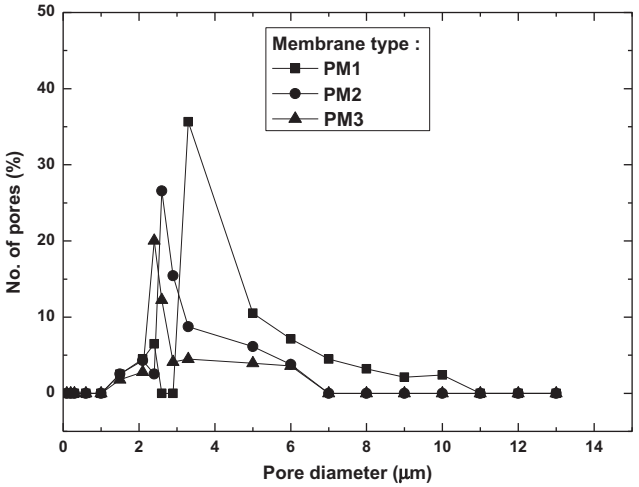

Fig. 3. FESEM based pore size distributions of PM1, PM2 and PM3 membranes.

9.25×10^{-3}, 2.61 to 7.76×10^{-3} and 1.64 to 5.05×10^{-3} m^3/m^2 s with a variation in applied pressures from 68.9 to 206.70 kPa for PM1, PM2 and PM3 membranes, respectively. The obtained pure water flux is about 4 times higher than the pure water flux reported by Nandi et al. [11]. The average membrane porosity was obtained using the Archimedes's principle and its variation with fabrication pressure is shown in Fig. 4b. It can be observed that the membrane porosity reduced from 37.4% to 30.1% with an increase in fabrication pressure from 25 to 73 Mpa, thus indicating that higher fabrication pressure enabled the reduction in porosity by 7%. The average pore size of the membrane determined using average porosity and hydraulic permeability is also presented in Figs. 4b for all the membranes. The average pore size of the membranes varied from 3.06 μm to 2.16 μm, which is significantly higher than the average pore size of 0.6 μm reported by Nandi et al. [11] using the paste method. Therefore, the utilization of water during the paste method enabled finer arrangement of the precursors in the paste which is not the case for the uniaxial dry compaction method. While this is true and can be predicted even without doing the fabrication experiments, it is important to conceive technically the role of water in the paste method and the fabrication pressure in the dry compaction method to influence membrane morphology. In other words, the elimination of water as a binding agent during green mold membrane fabrication strongly enhances the membrane pore size. Thus, more research is required to relate laboratory fabrication techniques with extrusion based ceramic membrane fabrication.

Fig. 5a–c presents the time dependent flux for membranes PM1, PM2 and PM3 respectively at various values of transmembrane pressure (ΔP) during dead end MF of oil–water emulsion. It can be observed that for all the membranes higher ΔP provides higher flux. Further, a significant variation in the near steady state membrane flux is contributed due to the variation in membrane morphology. For instance, at an operating ΔP of 206.7 kPa, the membrane flux after 30 min of dead end MF is about 24×10^{-6}, 11×10^{-6} and 8×10^{-6} m^3/m^2 s for PM1, PM2 and PM3 respectively. It

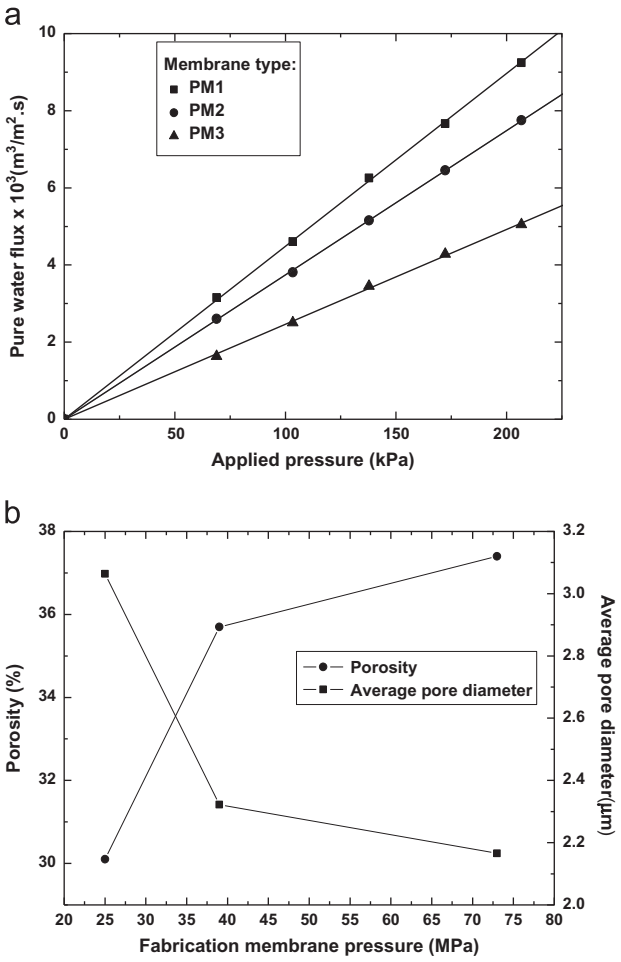

Fig. 4. (a) Variation of pure water flux with applied pressure for the membranes PM1–PM3 and (b) dependence of membrane porosity and average pore size on fabrication pressure.

can also be observed that the time dependent membrane flux varied from 124 to 24×10^{-6}, 96 to 11×10^{-6}, 86 to 8×10^{-6} m^3/m^2 s for PM1, PM2 and PM3 respectively, at a ΔP of 206.7 kPa at the end of 30 min of operation. Therefore, it is apparent that the membrane morphology significantly influences the near steady state flux but not the intial flux. This is probably due to the reason that the membranes fabricated at lower fabricating pressures possessed wider pore size distributions and are less susceptible for lower fouling and hence membrane PM1 is the optimal in terms of membrane flux.

The variation in time dependent oil rejection for various membranes and at various ΔP is presented in Fig. 6a–c. As shown, the membrane rejection varies almost linearly for PM3 membrane with time and slightly non linear for the PM1 membrane. This indicates that pore blocking could be significant for the PM1 membrane but need not be the case for PM3 membrane. It is also observed that the rejection decreases with increasing ΔP for all the membranes. This is due to the reason that higher pressures facilitate the enhancement of wetting and coalescence of oil droplets and could enable some oil droplets to pass through the membrane pores to reach the permeate stream. The enhancement in rejection with time for

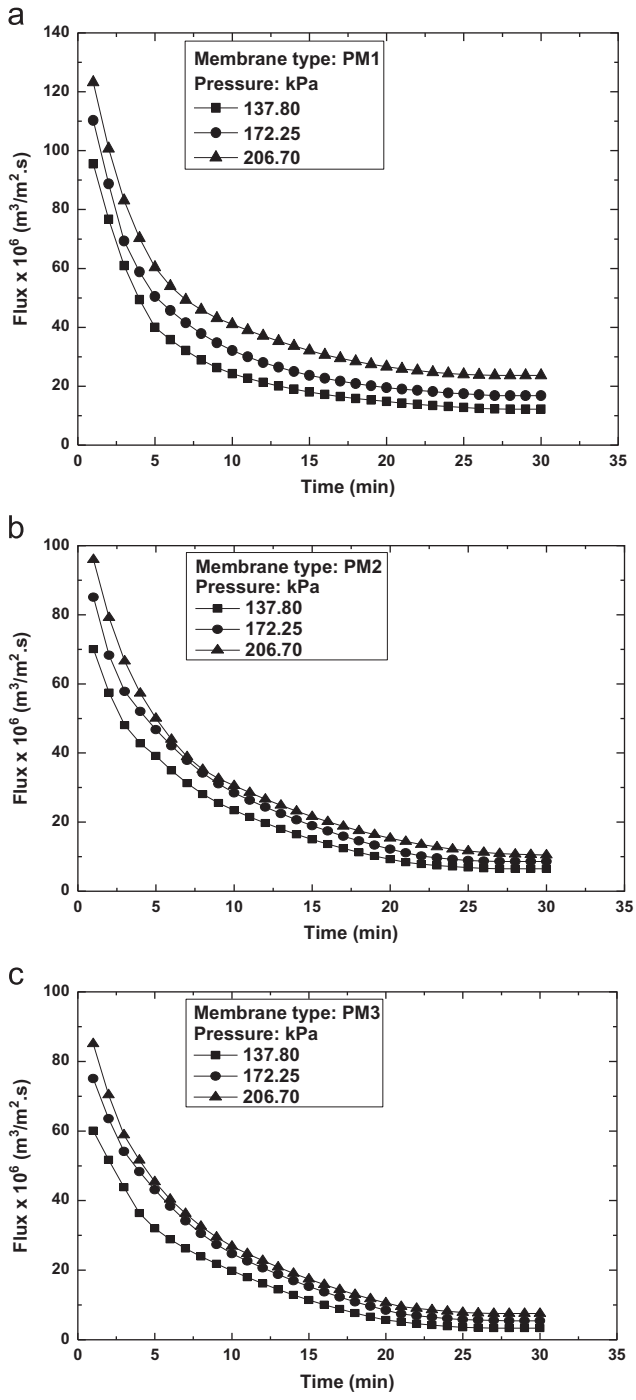

Fig. 5. Variation of time dependent flux with pressure for (a) PM1 (b) PM2 and (c) PM3 membranes.

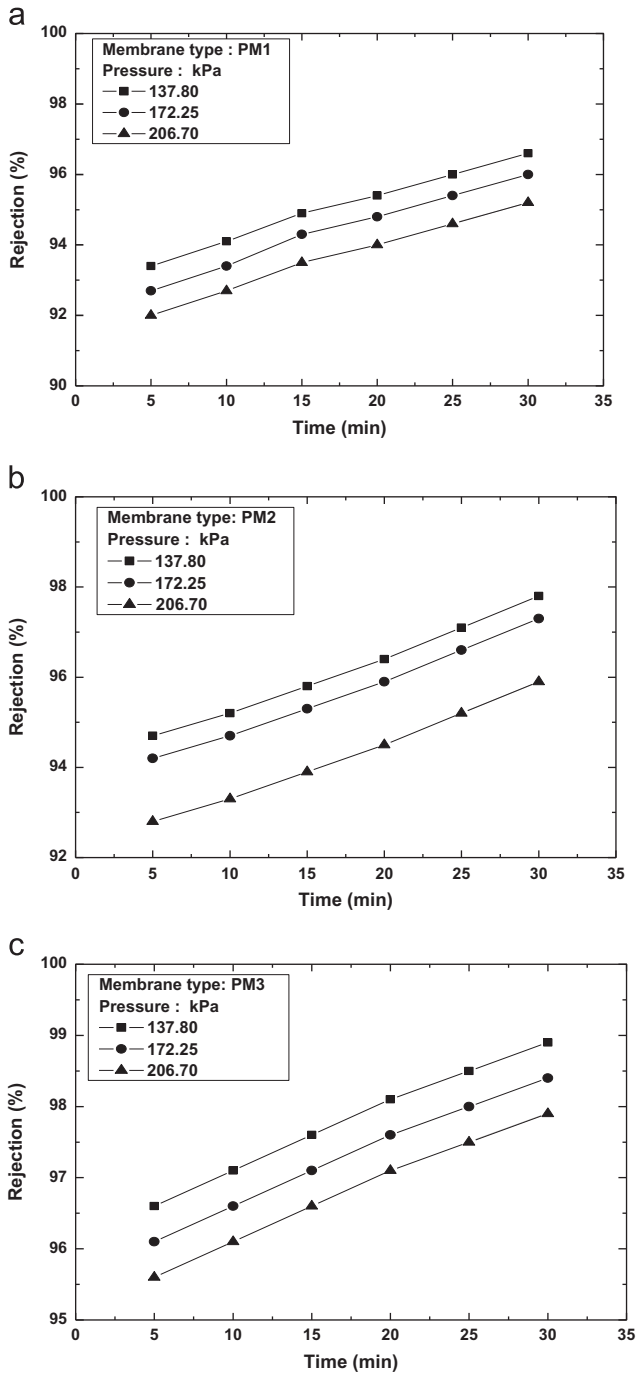

Fig. 6. Variation of rejection with time at various pressures for (a) PM1 (b) PM2 and (c) PM3 membranes.

all the membranes is because of reduction of the pore size due to pore blocking and adsorption of oil droplets on the pores. For membrane PM1, the rejection varied from 93.4% to 96.6% at a ΔP of 137.80 kPa which reduced to 92%–95.2% at a ΔP of 206.70 kPa. The insignificant reduction in ejection at higher ΔP during MF is indicative towards satisfactory permeation of the membranes.

For a ΔP variation from 137.8 to 206.8 kPa, the fouling indices for various membranes are evaluated to vary from 40.06% to 29.40%, 31.73% to 25.26% and 25.14% to 15.54% for membranes PM1, PM2 and PM3 respectively. Considering fouling index as an additional criterion for the selection of membranes, the membrane PM3 at a ΔP of 206.70 kPa is the optimal choice to process the choosen feed. In other words this membrane with a fouling index of 15.54% and a near steady state flux of 8×10^{-6} m^3/m^2 s and a rejection of 97.6% is the most suitable for the treatment of oil water emulsions. For all membranes, lower ΔP (137.80 kPa) is not recommendable for MF operations. A comparative assessment of the obtained membrane permeability and rejection of the PM3 membrane is

Table 1
Comparison of obtained flux and rejection values for PM3 membrane with those available in the literature.

S. no.	Author	Average membrane properties		Feed concentration (mg/L)	Time (min)	Membrane permeability (m^3/m^2 s kPa)	Pressure differential (kPa)	Rejection
		Pore size (μm)	Porosity (%)					
1.	Vasanth et al.[7]	1.30	30	125	30	2.21×10^{-6}	276.4	85%
2.	Monash et al.[6]	0.98	44	200	30	2.31×10^{-7}	345.4	96%
3.	Nandi et al. [5]	0.55	42	50	30	3.28×10^{-7}	41.37	97.3%
4.	Vasanth et al. [8]	1.21	26	200	30	3.39×10^{-8}	69.0	96%
5.	This work	2.16	37.4	400	30	3.65×10^{-8}	206.70	97.9%

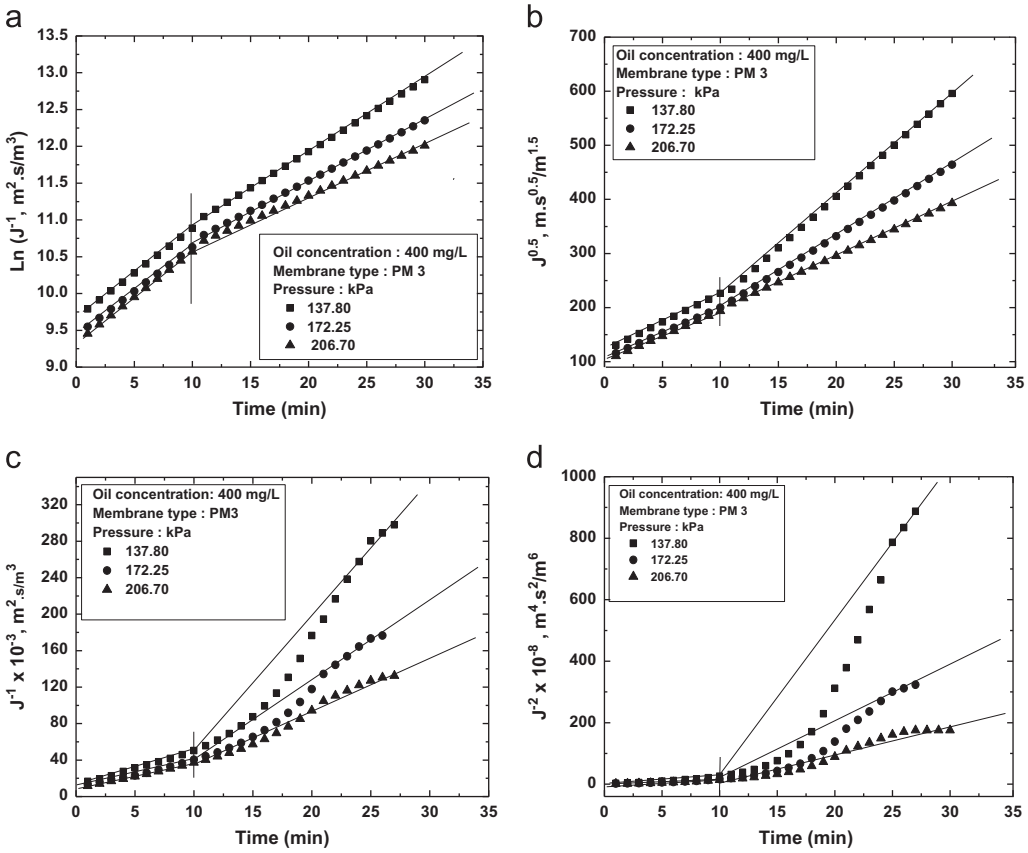

Fig. 7. Linearized plots for the fitness of various pore blocking models to represent flux decline data for membrane PM3 at a ΔP of 206.7 kPa. (a) Complete pore blocking, (b) standard pore blocking, (c) intermediate pore blocking, and (d) cake filtration.

conducted with the data available in the literature and is presented in Table 1. It can be observed that the obtained permeability and rejection for PM3 membrane are comparable with the values presented in the literature and the higher pore size of the membrane could process feeds with relatively higher concentration of oil (400–500 mg/L).

For the obtained flux decline data, the single pore blocking model is considered and the RMS error is calculated. It is seen that the RMS error varied from 36.66% to 11.06%, 6.46% to 5.31%, and 11.73% to 6.41%, for membranes PM1, PM2 and PM3, respectively. Also the RMS errors for both the cases namely the most competent single pore blocking model and the most competent combination model are 30% and 6%, respectively.

Fig. 7 presents the linearized plots for the fitness of various pore blocking models (cake filtration, intermediate pore blocking, standard and complete pore blocking) for PM3 membrane at various values of ΔP during the dead end MF. It can be observed that even the consideration of a single model in a combination based approach does not fit the flux decline data (Fig. 7c and d). Based on several permutations and combinations, the most competent combination of the model is identified using the correlation coefficient (R^2) values. Table 2 summarizes the fitness of combination models for various membranes at a ΔP of 206.70 kPa. It can be observed that the support pore size strongly influences pore blocking phenomena. For the PM1 membrane having wider pore size distribution, cake filtration model fits well to represent the data. On the other hand this membrane has a fouling index of 29.47%. Hence it is concluded that the onset of cake filtration need not indicate minimal reversible fouling and therefore

Table 2
Coefficient of regression (R^2) values for the most competent combination of various pore blocking models for all membranes (PM1–PM3) and all values of ΔP.

Membrane type	Pressure (kPa)	Complete pore blocking		Standard pore blocking		Intermediate pore blocking		Cake filtration	
		Intial	Final	Intial	Final	Intial	Final	Intial	Final
PM 1	137.80	0.962	0.949	0.988	0.964	0.997	0.975	0.976	0.987
	172.25	0.956	0.924	0.984	0.941	0.997	0.955	0.985	0.975
	206.70	0.950	0.906	0.976	0.919	0.991	0.931	0.994	0.950
PM 2	137.80	0.984	0.938	0.996	0.957	0.995	0.967	0.961	0.966
	172.25	0.982	0.939	0.996	0.954	0.996	0.962	0.964	0.960
	206.70	0.979	0.972	0.994	0.985	0.998	0.990	0.977	0.981
PM 3	137.80	0.980	0.949	0.995	0.968	0.998	0.970	0.972	0.943
	172.25	0.994	0.942	0.999	0.961	0.990	0.968	0.944	0.958
	206.70	0.986	0.933	0.998	0.952	0.997	0.962	0.961	0.963

generalized rules of thumb are always not applicable. On the other hand, for the PM3 membrane, the combination of standard pore blocking (during 1–10 min) and cake filtration (during 11–30 min) provide the best fitness toward representing the flux decline data. It is also important to note that PM3 membrane has a minimal fouling index of 15.54%. Therefore, while pore blocking could not be eliminated during initial stages of MF, the onset of cake filtration at a later stage is promising to give a lower fouling index of the PM3 membrane. In summary, it is apparent that MF experiments using membranes possessing wider pore size distribution, and feed stream with higher oil concentration (400 mg/L) did not indicate the flux decline phenomena to be represented with the single pore blocking model. In that case combinational models have to be considered to represent well the flux decline phenomena.

Fig. 8 summarizes the parity plot for the obtained data for two different cases namely the consideration of most competent single pore blocking and most competent combination models. It may be observed from Fig. 8a that for the first case significant number of data points deviated very much from the parity but for the second case (Fig. 8b), the deviation is minimal for the combination models.

Table 3a summarizes the model parameters for various membranes to represent the flux data (at ΔP of 206.7 kPa) as a combination of the two most competent pore blocking models. It can also be observed from the table that the RMS error values are 3.17–6.39%. Further, it is apparent that membrane morphology strongly influences the onset of various pore blocking phenomena. For instance, for the PM1 membrane having wider pore size distributions, the cake filtration model fits well which is the not case for PM3 membrane where the standard pore blocking model fits well in initial flux regime. Also, the instantaneous flux (J_0) for these membranes are evaluated as 1.58×10^{-6}, 9.16×10^{-6} and 82×10^{-6} m^3/m^2 s for PM1, PM2 and PM3 membranes respectively, which is 58.5, 8.4, and 61.5 times lower than the corresponding pure water flux of these membranes. This indicates that the membrane morphology profoundly influences the instantaneous flux and also morphology of the dynamic gel layer. The onset of cake filtration as a competent pore blocking for the PM1 membrane is possibly due to a very efficient instantaneous pore blocking that enables cake filtration to contribute to fouling later on wards. Thus, these observations definitively indicate the complexity involved in the interaction between adsorption of oil in the pores, pore blocking and associated dynamic gel layer morphology.

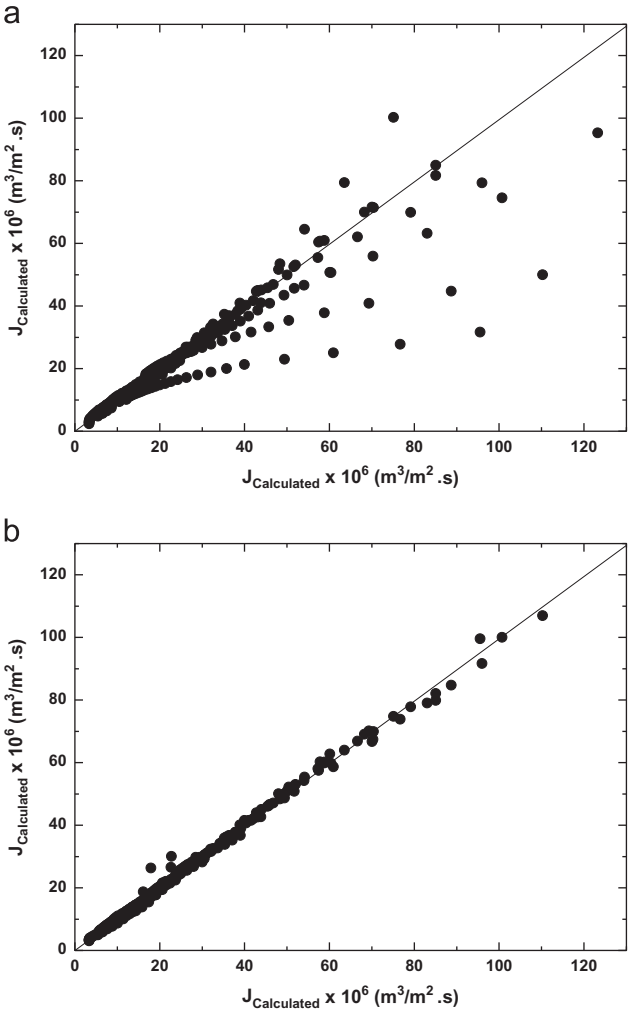

Fig. 8. Parity plots for the flux values for (a) most competent single pore blocking model and (b) most competent combination of pore blocking models for all membranes PM1–PM3.

Table 3a
Summary of model parameters for the best fit combination models for the flux data obtained for all the membranes at a ΔP of 206.7 kPa.

Membrane type	Intial		Final		RMSE (%)
	Type of model	Parameters	Type of model	Parameters	
PM 1	Cake filtration	$J_0=1.58\times10^{-4}$ m^3/m^2 s $k_c=2.00\times10^{-7}$ s m^{-2}	Cake filtration	$J_0=3.67\times10^{-5}$ m^3/m^2 s $k_c=2.15\times10^{-7}$ s m^{-2}	5.93
PM 2	Standard pore blocking	$J_0=9.16\times10^{-4}$ m^3/m^2 s $k_s=95.52$ m$^{-0.5}$ s$^{-0.5}$	Intermediate Pore blocking	$J_0=2.97\times10^{-5}$ m^3/m^2 s $k_i=5159$ m^{-1}	3.17
PM 3	Standard pore blocking	$J_0=8.20\times10^{-5}$ m^3/m^2 s $k_s=101.1$ m$^{-0.5}$ s$^{-0.5}$	Cake filtration	$J_0=1.17\times10^{-4}$ m^3/m^2 s $k_c=1.14\times10^{-7}$ s m^{-2}	6.39

Table 3b
Summary of model parameters for the best fit combination models for the flux data obtained for PM3 membrane at various values of ΔP.

Membrane type	Pressure (kPa)	Intial		Final		RMSE (%)
		Type of model	Parameters	Type of model	Parameters	
PM 3	137.80	Intermediate pore blocking	$J_0=6.27\times10^{-5}$ m^3/m^2 s $k_i=12{,}170$ m^{-1}	Intermediate pore blocking	$J_0=2.63\times10^{-5}$ m^3/m^2 s $k_i=13{,}176$ m^{-1}	6.80
	172.25	Standard pore blocking	$J_0=7.47\times10^{-5}$ m^3/m^2 s $k_s=106.3$ m$^{-0.5}$ s$^{-0.5}$	Intermediate pore blocking	$J_0=2.65\times10^{-5}$ m^3/m^2 s $k_i=58{,}446$ m^{-1}	6.68
	206.70	Standard pore blocking	$J_0=8.20\times10^{-5}$ m^3/m^2 s $k_s=101.1$ m$^{-0.5}$ s$^{-0.5}$	Cake filtration	$J_0=1.17\times10^{-4}$ m^3/m^2 s $k_c=1.14\times10^{-7}$ s m^{-2}	6.39

Table 3b summarizes the pore blocking model parameters that were obtained using the most competent combination of two pore blocking models for the PM3 membrane. It can be observed that the RMS error for the model fitness is within 6.3–6.8%. Further it may also be observed that ΔP influences the type of pore blocking mechanism. For instance, at a lower ΔP of 137.80 kPa, intermediate pore blocking occurred which transformed to standard pore blocking at a higher ΔP of 172.25 kPa and 206.70 kPa. The instantaneous flux values are varied about 55.1, 59.4 and 69.5 times lower than the corresponding pure water flux values. This indicates that ΔP insignificantly influences instantaneous membrane fouling and the dynamic gel layer morphology could be strongly affecting the rejection characteristics at higher pressure. The same is also evident from the rejection data and fouling behavior discussion in previous section.

5. Conclusion

This work addresses results attempting to visualize upon the role of the fabrication method in membrane morphology. It is observed that for a similar dry basis composition, the uniaxial method provides wider pore size distribution and pore sizes in comparison with the membrane fabricated with the paste method. Thus it will be even more interesting to examine the role of wet binding agents in altering the membrane morphology and pore size distributions and further experimentation. The membranes fabricated using the uniaxial dry compaction method at a fabrication pressure of 73 Mpa with the chosen precursor formulation possessed an average pore size and porosity of 2.16 μm, and of 37.4% respectively, and is the optimal choice to process 400 mg/L oil water emulsions. The membrane provides a near steady state flux of 8×10^{-6} m^3/m^2 s and a rejection of 97.9% at a ΔP of 206.70 kPa at which minimal fouling index of 15.54% is evaluated. For all the membranes, the combination model provides the best fitness in comparison with the most competent single pore blocking model. In summary, the membrane PM3 is promising for the treatment of oil water emulsion in the concentration range of 400–500 mg/L as a low cost ceramic membrane technology.

References

[1] F.L. Hua, Y.F. Tsang, Y.J. Wang, S.Y. Chan, H. Chu, S.N. Sin, Performance study of ceramic microfiltration membrane for oily wastewater treatment, Chemical Engineering Journal 128 (2007) 169–175.
[2] N. Saffaj, M. Persin, S.A. Younsi, A. Albizane, M. Cretin, A. Larbot, Removal of salts and dyes by low $ZnAl_2O_4$–TiO_2 ultrafiltration membrane deposited on support made from clay, Separation and Purification Technology 47 (2005) 36–42.
[3] M.R. Weir, E. Rutindeka, C. Detellier, C.Y. Feng, Q. Wang, T. Matsuura, R. Le Van Mao, Fabrication, characterization and preliminary testing of all inorganic ultrafiltration membranes composed entirely of a naturally occurring sepiolite clay mineral, Journal of Membrane Science 182 (2001) 41–50.
[4] Y. Dong, S. Chen, X. Zhang, J. Yang, X. Liu, G. Meng, Fabrication and characterization of low cost tubular mineral based ceramic membranes for

microfiltration from natural zeolite, Journal of Membrane Science 281 (2006) 592–599.
[5] B.K. Nandi, R. Uppaluri, M.K. Purkait, Treatment of oily wastewater using low cost ceramic membrane: flux decline mechanism and economic feasibility, Separation Science and Technology 44 (2009) 2840–2869.
[6] P. Monash, G. Pugazhenthi, Effect of TiO_2 addition on the fabrication of ceramic membrane supports: a study on the separation of oil droplets and bovine serum albumin (BSA) from its solution, Desalination 279 (2011) 104–114.
[7] D. Vasanth, R. Uppaluri, G. Pugazhenthi, Fabrication and properties of low cost ceramic microfiltration membranes for separation of oil and bacteria from its solution, Journal of Membrane Science 379 (2011) 154–163.
[8] D. Vasanth, R. Uppaluri, G. Pugazhenthi, Performance of low cost ceramic microfiltration membranes for the treatment of oil in water emulsions, Separation Science and Technology 48 (2013) 1–10.
[9] M. Abbasi, M. Mirfendereski, M. Nikbakht, M. Golshenas, T. Mohammadi, Performance study of mullite and mullite–alumina ceramic MF membranes for oily wastewaters treatment, Desalination 259 (2010) 169–178.
[10] E. Sriharsha, R. Uppaluri, M.K. Purkait, Preparation and characterization of low cost ceramic membranes for mosambi juice clarification, Desalination 317 (2013) 32–40.
[11] B.K. Nandi, R. Uppaluri, M.K. Purkait, Preparation and characterization of low cost ceramic membranes for micro-filtration applications, Applied Clay Science 42 (2008) 102–110.
[12] M. Ghaedi, B. Sadeghian, S.N. Kokhdan, A.A. Pebdani, R. Sahraei, A. Daneshfar, A. Mihandoost, Study of removal of Direct Yellow 12 by cadmium oxide nanowires loaded on activated Carbon, Materials Science and Engineering C 33 (2003) 2258–2265.
[13] M. Ghaedi, J. Tashkhourian, M. Montazerozohori, M. Soylak, Silver nanoparticle loaded on activated carbon and activated carbon modified with 2-(4-isopropylbenzylideneamino) thiophenol (IPBATP) as new sorbents for trace metal ions enrichment, International Journal of Environmental Analytical Chemistry 93 (4) (2013) 386–400.
[14] M. Ghaedi, M. Ghayedi, S.N. Kokhdan, R. Sahraei, A. Daneshfar, Palladium, silver, and zinc oxide nanoparticles loaded on activated carbon as adsorbent for removal of bromophenol red from aqueous solution, Journal of Industrial and Engineering Chemistry 19 (4) (2013) 1209–1217.
[15] J. Hermia, Constant pressure blocking filtration laws—application to power-law non-newtonian fluids, Transactions of the Institution of Chemical Engineers 60 (1982) 183–187.